Carbohydrate Polymers 116 (2015) 9–17

Contents lists available at ScienceDirect

Carbohydrate Polymers

journal homepage: www.elsevier.com/locate/carbpol

Green synthesis of the silver nanoparticles mediated by pullulan and 6-carboxypullulan☆

Sergiu Coseri[a,*], Alina Spatareanu[a], Liviu Sacarescu[a], Cristina Rimbu[b], Daniela Suteu[c], Stefan Spirk[d,e,**], Valeria Harabagiu[a]

[a] Petru Poni Institute of Macromolecular Chemistry of Romanian Academy, 41 A, Gr. Ghica Voda Alley, 700487 Iasi, Romania
[b] University of Agricultural Sciences and Veterinary Medicine, Faculty of Veterinary Medicine—UASVM Iași, Aleea Mihail Sadoveanu nr.8, 700489 Iași, Romania
[c] "Gheorghe Asachi" Technical University of Iasi, Faculty of Chemical Engineering and Environmental Protection, 71A Prof. Dr. Docent D. Mangeron Blvd, 700050 Iasi, Romania
[d] Graz University of Technology, Institute for Chemistry and Technology of Materials, Stremayrgasse 9, 8010 Graz, Austria
[e] University of Maribor, Institute for the Engineering of Materials and Design, Smetanova Ulica 17, 2000 Maribor, Slovenia

ARTICLE INFO

Article history:
Received 9 December 2013
Received in revised form 19 May 2014
Accepted 5 June 2014
Available online 12 June 2014

Keywords:
Pullulan
6-Carboxypullulan
TEMPO
Silver nanoparticles
Oxidation

ABSTRACT

Unoxidized and carboxylated pullulan (obtained by pullulan oxidation using TEMPO–sodium hypochlorite–sodium bromide system) have been used as mediators for the silver nanoparticles formation (AgNPs), under environment-friendly conditions: using aqueous solutions, room temperature and notably, by using both mediators as reducing and stabilizing agents. The formation of AgNPs was first screened by measuring the surface plasmon resonance peak in the range of 380–440 nm using UV–vis spectroscopy. The morphology of the synthesized silver nanoparticles was determined by TEM, which indicated that the AgNPs differ on shape and thickness of the polymer shell by varying the silver nitrate concentration, different size and shape of AgNPs was achieved. The presence of elemental silver and the crystalline structure of the AgNPs were confirmed by EDX and XRD analyses. Moreover, the possible functional groups of pullulan (oxidized pullulan) responsible for the reduction and stabilization of AgNPs were evaluated using FT-IR.

The results showed that both, pullulan and 6-carboxypullulan could be successfully used as reducing as well as capping agents for the AgNPs synthesis which shows potential antimicrobial activity against Gram positive and Gram negative bacteria.

1. Introduction

In the past decade, research on nanoscale materials has entered into the focus of many different areas since they exhibit unique chemical and physical properties (Garciá-Barrasa, López-de-Luzuriaga, & Monge, 2011), leading to manifold applications in biomedicine, electronics, biosensors, catalysis, and optics for instance (Alayoglu, Nilekar, Mavrikakis, & Eichhorn, 2008; Aslan, Lakowicz, & Geddes, 2005; Sapsford, Pons, Medintz, & Mattoussi, 2006). Of particular interest are nanoparticles, whose properties can be tuned by variation of their size, shape and surface functional groups. There is a huge variety of methods for the preparation of metal nanoparticles (MNPs) ranging from physical solid-state treatments (including milling, grinding and mechanical alloying techniques) (Pimpang, Sutham, Mangkorntong, Mangkorntong, & Choopun, 2008; Salah et al., 2011), gas-phase synthesis (e.g. high-temperature evaporation (Zschech et al., 2006), laser ablation (Giorgetti, Giusti, Laza, Marsili, & Giammanco, 2007), pyrolysis (Turner et al., 2010), plasma synthesis (Ko et al., 2006) to liquid-phase synthesis. The latter includes a variety of methods such as co-precipitation, microemulsifying, microwave irradiation, solvothermal treatments, sol–gel syntheses, for instance (Breitwieser et al., 2013; Khan, Al-Thabaiti, Obaid, & Al-Youbi, 2011; Khorsand Zak, Razali, Abd Majid, & Darroudi, 2011; Kowlgi, Lafont, Rappolt, & Koper, 2012; Sharmaa, Sharmab, Kaitha, Rajputa, & Kaurb, 2011; Wu et al., 2011; Xu et al., 2007).

☆ Paper dedicated to the 65th anniversary of "Petru Poni" Institute of Macromolecular Chemistry of Romanian Academy, Iasi, Romania.

* Corresponding author at: Petru Poni Institute of Macromolecular Chemistry of Romanian Academy, Natural Polymers, 41A Gr. Ghica Voda Alley, 700487 Iasi, Romania. Tel.: +40 232 217454/+43 316 873 32284; fax: +40 232 211299/+43 316 873 32301.
** Corresponding author at: Graz University of Technology, Institute for Chemistry and Technology of Materials, Stremayrgasse 9, 8010 Graz, Austria.
E-mail addresses: coseris@icmpp.ro (S. Coseri), stefan.spirk@tugraz.at (S. Spirk).

http://dx.doi.org/10.1016/j.carbpol.2014.06.008
0144-8617/

In all of the afore mentioned methods, the chemical reduction of metal salt precursors to the elemental metal nanoparticles plays a crucial role. In general, the chemical reduction of metal salts requires a reducing agent and a stabilizer one, in order to obtain shape- and size-controlled MNPs. In the case of silver, the most widely used precursor is silver nitrate ($AgNO_3$). Usually, the generation of Ag nanoparticles involves three steps, namely the reduction reaction of silver ions to free silver atoms, nucleation and growth. Since the kinetics of the reduction reaction plays a large role for the nucleation and growth stage (Garciá-Barrasa et al., 2011) an impressive number of reducing agents (e.g. $NaBH_4$, citric acid, ascorbic acid etc) and capping agents (e.g. oleylamine, cetyltriethylammonium bromide, poly(vinylpyrrolidone) etc.) have been described in literature (Garciá-Barrasa et al., 2011; Song, Lee, Park, & Lee, 2009).

A new concept has recently been introduced commonly referred as "*green*" synthesis where the used solvents and chemicals are being non-toxic and benign compounds to the environment. Raveendran et al. (2003) reported as early as 2003, the completely "*green*" synthesis and stabilization of silver nanoparticles, by using water as solvent, β-D-glucose as a reducing agent and starch for the stabilization of the resulted nanoparticles. In this way, the authors reported the formation of 5 nm AgNPs. Since then, a large number of polysaccharides were used as renewable polymers able to stabilize the AgNPs (Huang & Yang, 2004; Ifuku, Tsuji, Morimoto, Saimoto, & Yano, 2009; Raveendran, Fu, & Wallen, 2003; Tran et al., 2010; Twu, Chen, & Shih, 2008). Very recently, the synthesis of silver nanoparticles with sizes in the 2–40 nm range by using pullulan as both a reducing and stabilizing agent has been accomplished at rather high temperature (121 °C). The formation of AgNPs has been demonstrated by the appearance of the surface plasmon resonance (SPR) transition in the visible region of 400–450 nm. Likewise, it was shown that an increase in the silver nitrate concentration leads to a substantial increase in the SPR band (Kanmani & Taik Lim, 2013). Besides applications in nanotechnology, silver has been used for ages in the treatment of infections and wounds. Recently, upcoming resistances of pathogens against antibiotics (particular in medical care) led to an increase of silver incorporation into medical materials and currently a variety of applications are on the market (AQUACEL®, SILVERCEL™).

In the present study, pullulan has been oxidized by employing the 2,2,6,6-tetramethylpiperidin-1-yl radical (TEMPO)–sodium hypochlorite–sodium bromide system, to convert primary OH groups of pullulan to carboxylic functions. The goal of this functionalization was the introduction of carboxylic groups into the pullulan backbone. As a consequence, the negatively charged carboxylic groups allow for a better stabilization of the silver nanoparticles due to the electrosteric stabilization. Subsequently, the syntheses of silver nanoparticles are described in the presence of the pullulan or oxidized pullulan as both reducing and stabilizing agents using water as solvent at room temperature. Finally, the silver nanoparticles will be tested against their activity to act as antimicrobial agents towards *Staphylococus aureus* and *Escherichia coli* strains.

2. Materials and methods

2.1. Materials

Pullulan (M_w = 150 kDa) purchased from TCI Europe was dried under vacuum at 100 °C overnight prior to use 2,2,6,6-tetramethylpiperidin-1-yl (TEMPO) 99% Sigma-Aldrich, sodium hypochlorite (NaOCl, 9% chlorine, Chemical Company Romania) and sodium bromide (99% Alfa Aesar) were used as received. Silver nitrate (≥99.0%) was purchased from Sigma-Aldrich and used without further purification. All solutions were prepared using ultra-filtered high purity deionized water.

2.2. Pullulan oxidation

Pullulan (0.25 g) was dissolved in deionized water (40 mL) at room temperature. After complete dissolution, TEMPO (5 mg) and NaBr (25 mg) were added under rigorous stirring. A 9% sodium hypochlorite solution (2.1 mL) was adjusted to pH 10 using 2 M HCl, and the resulting solution was slowly added to the pullulan solution. The pH was monitored by a pH meter and maintained at 10 by addition 0.2 M sodium hydroxide solution. After 4 h, the reaction was stopped by quenching the unreacted NaOCl with methanol (2.5 mL), and then acidified to a pH around 6.8. In the next step, the reaction mixture was precipitated using ethanol and subjected to centrifugation. After centrifugation, the solid was redissolved in water, and the resulted solution was desalted and the oligomers were removed by dialysis. Dialysis was performed against water in a 4 L beaker using dialysis tubing from polyethersulfone (cut-off: 10,000 g cm^{-1}) for four days, replacing the water twice each 24 h. The oxidized pullulan was then recovered by freeze-drying.

2.3. FTIR measurements

Infrared absorption spectra of pullulan and oxidized pullulan samples, as well as of the AgNPs, were recorded using a Bruker Vertex 70 spectrometer at a scan range from 4000 to 650 cm^{-1}, at a resolution of 2 cm^{-1} and 32 scans. The dried samples was powdered by grinding with KBr pellets and pressed into a mold.

2.4. NMR determinations

^{1}H-NMR and ^{13}C-NMR analyses of original and oxidized pullulan were performed by dissolving 10 mg or 50 mg, respectively, in 0.7 mL of D_2O. The obtained solution was filtered through a pipette containing glass wool into a standard 5 mm NMR tube. The NMR spectra were obtained on a Bruker Avance DRX 400 MHz Spectrometer, equipped with a 5 mm QNP direct detection probe and *z*-gradients.

2.5. Experimental procedure of the silver nanoparticles (AgNPs) preparation

Four sets of experiments for the AgNPs preparation were performed, by varying the silver nitrate ($AgNO_3$) concentration (0.01, 0.05, 0.1 and 0.5 M, respectively) and also by changing the pullulan with 6-carboxy pullulan as reducing agent as well as stabilizer used for the silver nanoparticles. In a typical run, 150 mL aqueous solution of biopolymer (0.5 wt%) was placed in a 500 mL three necks flask (protected against light by aluminum foil), and 9 mL fresh solution of $AgNO_3$ was added drop wise, keeping vigorous stirring at room temperature. After 6 h, the solutions turned pale yellow, and the mixture was centrifuged. The supernatant was dialyzed against water for two days, and then, the solid was recovered by freeze-drying.

2.6. Characterization of AgNPs

The AgNPs prepared by using pullulan or 6-carboxypullulan were characterized by using ultraviolet–visible (UV–vis) spectroscopy, FTIR, transmission electron microscopy (TEM), X-ray diffraction (XRD). The optical absorption properties of AgNPs samples were measured using a SPECORD 200 Analytik Jena spectrometer over the range of 300–700 nm. Zeta potential (ζ) was measured by using a dynamic light scattering technique (Zeta sizer model Nano ZS, Malvern Instruments, UK) with red laser 633 nm

(He/Ne). The average particle size was measured also based on the DLS analysis.

Zeta Potential (ζ) was calculated from the electrophoretic mobility (μ) determined at 25 °C. For $k\alpha \gg 1$ (k—Debye–Hűckel parameter and α—particle radius), the Smoluchowski relationship was used in the following equation:

$$\xi = \frac{\eta\mu}{\varepsilon} \quad (1)$$

where η is the viscosity and ε is the dielectric constant.

The apparent hydrodynamic diameter (D_H) of pullulan, oxidized pullulan and their silver nanoparticles aqueous solutions was determined through dynamic light scattering measurements by using Zetasizer ZS apparatus during the same experiment of zeta potential evaluation. The system uses a non-invasive back scatter (NIBS) technology, which reduces the multiple scattering effects. This Mie method is applied over the whole measuring range, situated in the range of 0.6 nm to 6 μm. The Eq. (2) was used to obtain the z-average distribution of the apparent hydrodynamic diameter (D_H) of the aggregates:

$$D_H = \frac{kT}{3\pi\eta D} \quad (2)$$

where D_H is the hydrodynamic diameter, k is the Boltzman constant, T is the temperature, η is the viscosity, D is the diffusion coefficient. It is worth to note that this mean size (hydrodynamic diameter) is intensity mean, being calculated from a signal intensity and is not a mass or number mean. The results presented good reproducibility with the deviation of the average diameter within 5%. The temperature was maintained constant at 25 °C (±0.1 °C) with a Peltier device.

TEM images were acquired with a Hitachi High-Tech HT7700 electron microscope (Hitachi High-Technologies Corporation, Tokyo, Japan), by using a drop of AgNPs aqueous solution directly placed onto a carbon-coated copper grid and allow to dry prior the TEM analysis. No staining is required for the sample preparation for this kind of instrument, due to the new high resolution objective lens which is incorporated into this apparatus (http://hitachi-hta.com/sites/default/files/literature/HT7700-EXALENS-HTD-E207.pdf). The particle size distribution was evaluated using the UTHSCSA Image Tool Version 3.00 program (UTHSCSA Dental Diagnostic Science, San Antonio, TX, USA). The energy dispersive X-ray analysis (EDX) was performed on the Quanta 200 (FEI) electron microscope equipped with EDX system. The crystal structure of the AgNPs was determined using an X-ray diffractor, (D8 Advance Bruker), with data acquisition taken at 0.02° s^{-1} by the reflection method. The operated voltage was 30 kV and the current was 36 mA.

2.7. Determination of antibacterial activity of AgNPs

The silver nanoparticles were tested using the agar well diffusion method. All the glassware, media and reagents used were sterilized in an autoclave at 121 °C for 30 min. *S. aureus* (ATCC 25923) *E. coli* (ATCC 25922) were used as a model test strains for Gram-positive and Gram-negative bacteria, respectively. These bacterial strains were aseptically inoculated overnight, at 37 °C into tryptic soy broth and brain heart infusion broth. Cells from different pathogens (1 mL) were added to tryptic soy agar and brain heart infusion broth media (100 mL) prior to plating and wells were made using an agar well borer. AgNPs (5 μg) were then added to the center well, and the plates were incubated at 37 °C for 24 h. Zone of inhibition were determined by measuring the diameter of the bacterial growth inhibition zone. Three independent experiments were carried out with each strain.

3. Results and discussion

3.1. Synthesis and characterization of 6-carboxy pullulan

Pullulan has been selectively oxidized by using TEMPO/sodium hypochlorite/sodium bromide system at room temperature for 4 h to convert the primary OH groups to carboxylic moieties. Under these conditions, more than 90% of the primary OH groups are converted to COOH (Spatareanu et al., 2014). Only catalytic amounts of TEMPO have been used, and the oxidant has been regenerated by $^{-}$OCl/HOCl at pH 10. During oxidation, TEMPO is converted to the nitrosonium ion, which is the actual oxidant, see Fig. 1.

^{13}C-NMR spectra of the original and oxidized pullulan are shown in Fig. 2. The spectrum (a) is characteristic for this polysaccharide and fits well to already report ^{13}C NMR data in literature (Paris & Stuart, 1999). In the case of pullulan, the two signals at 69.26 ppm and 63.19 ppm can be assigned to the C6 atom (6g1 → 4) and the primary C6 atom (4g-unit), which is capable to be oxidized. All signals can be unambiguously assigned (C1: 100.68–102.99 ppm, C4: 80.56 ppm and C2,3,5: 72.26 to 76.21 ppm). After 4 h of oxidation (sample OxPu 4), a decrease of the C6 (4g-unit) is observed, which is accompanied by the appearance of a new peak at 175.62 ppm, corresponding to a quaternary C atom of a COOH group. In order to assess the degree of oxidation (DO), proton NMR spectra have been acquired. The NMR technique is a valuable tool to assess the degree of substitution for pullulan functionalized products. Thus, Paris et al. reported back in 1995 the evaluation of the degree of oxidation of pullulan by using TEMPO as oxidizing agent (Paris & Stuart, 1999). The degree of esterification of water-soluble pullulan with cinnamic acid was also determined by using ^{1}H-NMR (Kaya et al., 2008). Very recently, Edgar et al., used ^{1}H-NMR technique to calculate the degree of substitution values of a series of 6-carboxypullulan ethers obtained by reaction of 6-carboxypullulan Na salt with tetrabutylammonium salt, follow by etherification with alkyl bromides and iodobutane (Pereira, Mahoney, & Edgar, 2014). The integration of the peaks in the range between 3.5 and 4.4 ppm and 5.35 and 5.45 ppm in the ^{1}H-NMR spectrum yield a DO of ca. 90% (Spatareanu et al., 2014).

3.2. Synthesis and characterization of AgNPs

The formation of AgNPs by the reduction of silver ions to silver metal species was achieved in the presence of aqueous solutions of pullulan or oxidized pullulan at room temperature over a period of 6 h. Four sets of experiments were carried out for each biopolymer (pullulan or oxidized pullulan) whereby the silver nitrate concentration was chosen to be in the final solution, 0.01, 0.1, 0.05 and 0.5 M, respectively. In the course of the preparation of the AgNPs, the initial colorless solution turned yellowish-brown as a result of the formation of silver nanoparticles. In the first step, the silver ions are reduced by the available reducing end groups of the pullulan (or oxidized pullulan). The resulted atoms form clusters that subsequently act as nucleation centers as soon as their concentration reaches a certain point. These nucleation centers in turn grow and form larger aggregates until all small aggregates are consumed. The surface ions are subsequently reduced, the aggregation process does not cease until larger particles are formed. However, the interaction of these particles with the polymer matrix would prevent further coalescence (Goia, 2004). An illustration of the silver nanoparticles coated by pullulan and oxidized pullulan is shown in Fig. 3.

The intrinsic structure of pullulan carrying multiple hydroxyl groups confers a protective and highly functionalized shell for nanoparticles. The supramolecular associations created by hydrogen bonds are able to coordinate to Ag providing stability for a longer period of time (steric stabilization). Moreover, in the case of

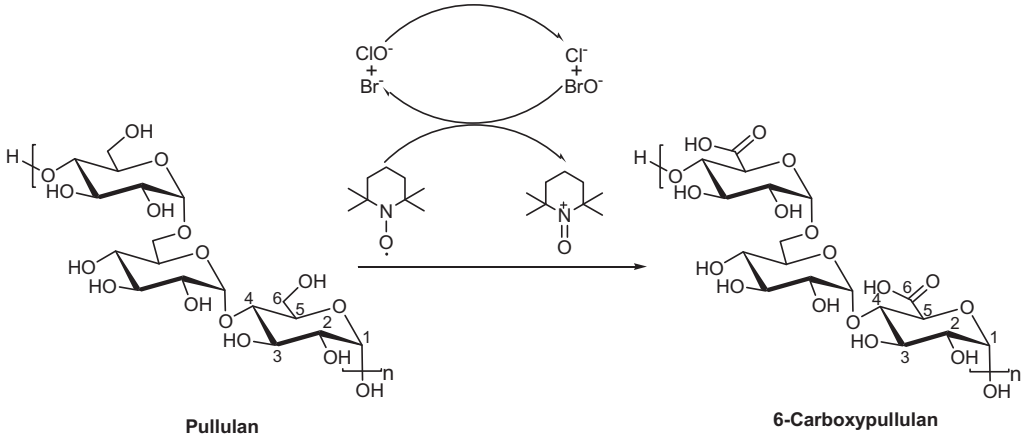

Fig. 1. Simplified scheme of TEMPO-mediated oxidation of pullulan.

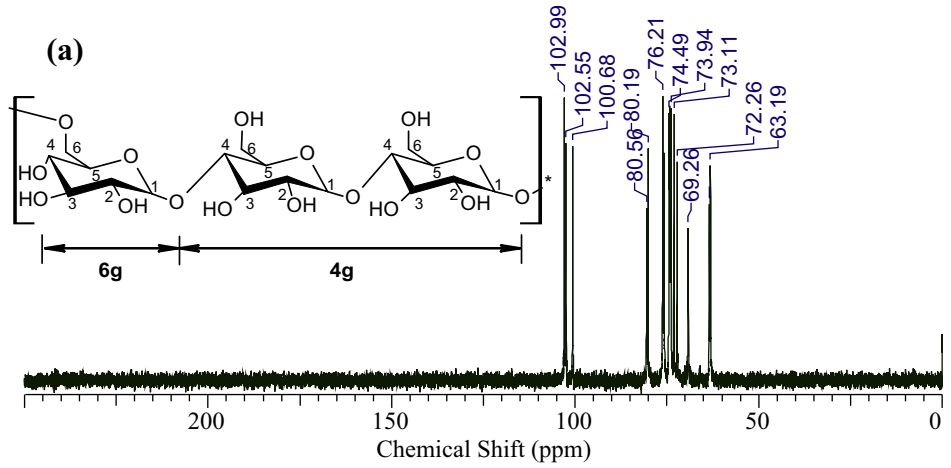

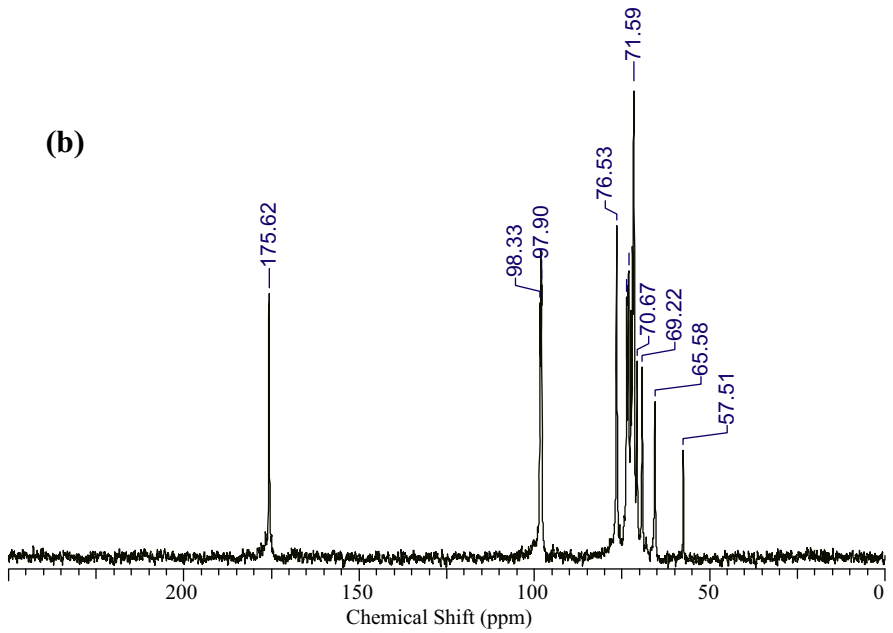

Fig. 2. ^{13}C-NMR spectra of pullulan (a), and OxPu 4 (b).

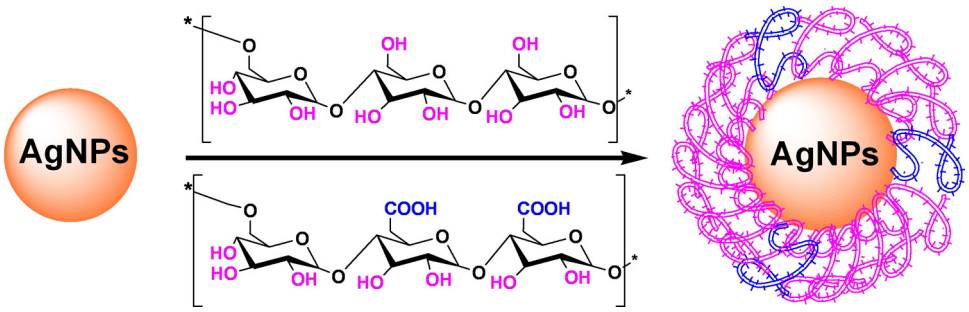

Fig. 3. Illustration of the silver nanoparticles formation mediated by pullulan or oxidized pullulan.

Table 1
Sample codes and zeta potential (ζ), determined at 25 °C, and pH = 6.6, for the AgNPs synthesized using pullulan and oxidized pullulan as reducing/stabilizing agents.

Sample code	Reducing/stabilizing agent	$AgNO_3$ conc. (M)	ζ (mV)
AgPu 0.01	Pullulan	0.01	−0.35 ± 0.1
AgPu 0.05	Pullulan	0.05	−3.46 ± 0.2
AgPu 0.1	Pullulan	0.1	−2.2 ± 0.2
AgPu 0.5	Pullulan	0.5	−4.3 ± 0.3
AgOxPu 0.01	Oxidized pullulan	0.01	−25.6 ± 0.3
AgOxPu 0.05	Oxidized pullulan	0.05	−37.4 ± 0.5
AgOxPu 0.1	Oxidized pullulan	0.1	−32.2 ± 0.4
AgOxPu 0.5	Oxidized pullulan	0.5	−34.4 ± 0.6

6-carboxypullulan the introduction of COOH groups will determine electrostatic repulsion between the negatively charged core–shell nanoparticles, an effect commonly referred to as electrosteric stabilization. The difference between those samples in terms of stability can be clearly seen by the zeta potential of the AgNPs. The silver nanoparticles encapsulated by oxidized pullulan exhibit higher negative zeta potential, indicating rather high stability. In contrast, the AgNPs surrounded by unmodified pullulan lead to rather neutral particles with a slightly negative zeta potential. An overview is summarized in Table 1.

The effect of the reducing/stabilizing agent on the AgNPs formation is illustrated by recording the UV–vis spectra, Fig. 4. It is well known that silver nanoparticles absorb radiation in the visible region of the electromagnetic spectrum (380–450 nm) due to the SPR transition (Bankura et al., 2012; Pandey, Goswami, & Nanda, 2012). The UV–vis absorption spectra of the silver nanoparticles are dependent on many factors, such as the size and shape of the nanoparticles, the silver precursor concentration, as well as the structure of the polymer used for the stabilizing the nanoparticle. As expected, the differences on the macromolecular backbone structures of pullulan and oxidized pullulan (obtained through the replacement of 90% of CH_2—OH groups from native pullulan by COOH moieties), used as stabilizer in this study will induce variations of the absorption maximum, i.e. 420 nm for oxidized pullulan vs. 424 nm for native pullulan). These differences originates in opposite nature of the two biopolymers: one uncharged polysaccharide (pullulan) and another one, highly negatively charged (oxidized pullulan), which essentially trigger different reducing and stabilizing activity. The lower concentrations of silver nitrate added to the pullulan/oxidized pullulan solutions, will shift the surface Plasmon resonance band toward lower wavelengths, (see Supplementary content associated with this paper) which indicates that the size and size distribution were decreased. The maximum absorption peak however, was observed at highest silver nitrate concentration used in this study (samples AgPu 0.5 and AgOxPu 0.5). Additionally, the UV–vis spectra of the same samples were recorded after six months of storage at room temperature (Fig. 4b). The SPR band of the AgOxPu 0.5 sample red shifted with only 4 nm,

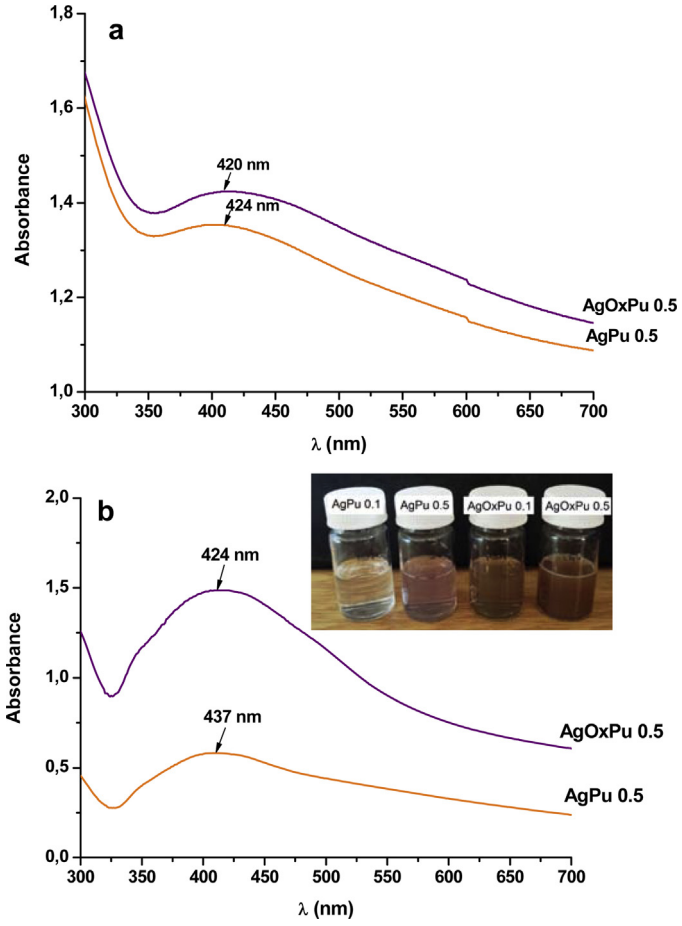

Fig. 4. The UV–vis spectra of the silver nanoparticles during synthesis (a), and after six months storage at room temperature (b).

whereas the AgPu 0.5 sample exhibit a SPR band red shifted with 13 nm. These observations suggest that oxidized pullulan could be a better stabilizing agent for AgNPs than pullulan, when the agglomeration is more pronounced.

The differences in the UV–vis absorption are related also with to the difference in the size of the corresponding nanoparticles. The TEM images (Fig. 5) clearly reveal that the size of the nanoparticles depend on the polysaccharide used for reduction. As expected, in case of the use of unmodified pullulan as stabilizer, the silver nanoparticles form larger aggregates (50–55 nm) than those stabilized by the oxidized pullulan (8 to 25 nm). The shape of the particles is spherical and in all cases the polysaccharide shell can be visualized by TEM. A rather large nanoparticle with a thick shell is depicted in Fig. 5a. In the second picture, Fig. 5b, the AgNPs have been interestingly obtained, in a higher extent as “twins”

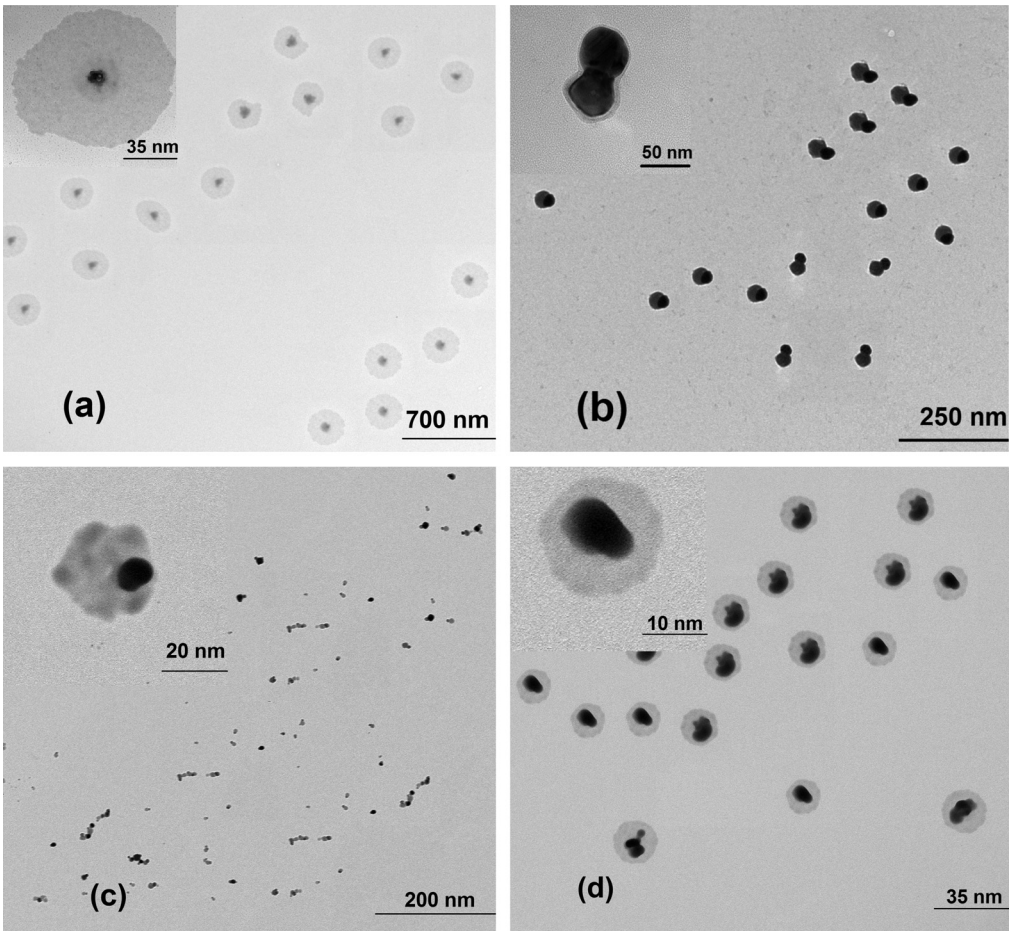

Fig. 5. TEM images of the AgPu 0.1 (a), AgPu 0.5 (b), AgOxPu 0.1 (c), and AgOxPu 0.5(d) samples (insets are shown individualized nanoparticles).

nanoparticles structures. For the oxidized pullulan–silver nanoparticles, the obtained structures are much smaller but the polysaccharide shell is still present (Fig. 5c and d). For the pullulan stabilized silver nanoparticles, the mean size of the particles increased by increasing the silver nitrate concentration, ranging from 30 nm in the case of sample AgPu 0.01 to 55 nm for the sample having the highest silver nitrate concentration (AgPu 0.5). Similarly, the mean size of the AgOxPu 0.01 nanoparticles as determined by TEM is only 8 nm, increasing gradually once the $AgNO_3$ is enlarged: 15 nm for the sample AgOxPu 0.05, 20 nm for the sample AgOxPu 0.1 and 25 nm for the sample AgOxPu 0.5, respectively.

Dynamic light scattering analyses of the colloidal solutions of the synthesized nanoparticles samples were carried out, showing reasonable PDI values, ranging from 0.106 in the case of AgPu 0.5 sample, to 0.55 for the AgOxPu 0.01 sample, which denote a narrow polydispersity. The diameter observed by DLS measurements varied from 233 nm in the case of pullulan-mediated silver nanoparticles, to 80 nm for those prepared by using oxidized pullulan, (sample AgOxPu 0.01, Fig. 6). These results clearly differ on those obtained by using TEM measurements. The differences are mainly due to the processes involved in the preparation of the samples. TEM technique uses the dry state of the sample to determine its particle size, whereas DLS method implies the measurement of the particle size in the hydrated state. Therefore we can assume that the size obtained by TEM is the actual size of the nanoparticle, since the diameter measured by the light scattering method is a hydrodynamic diameter, which appears always overestimate due to the strong interactions between solvent and nanoparticles constituents, especially hydrophilic biopolimers such as pullulan or its oxidized form (Gao et al., 2008). The hydrodynamic diameter as determined by DLS measurements increased also by increasing the silver precursor concentration, Fig. 6. Besides the factors linked by samples preparation for TEM and DLS analyses, discussed above, we can't rule out the aggregation phenomena appeared at high loading $AgNO_3$ for the AgNPs preparation, which are less probable to occur for the samples obtained in diluted solutions of $AgNO_3$ (0.01 and 0.05 M $AgNO_3$).

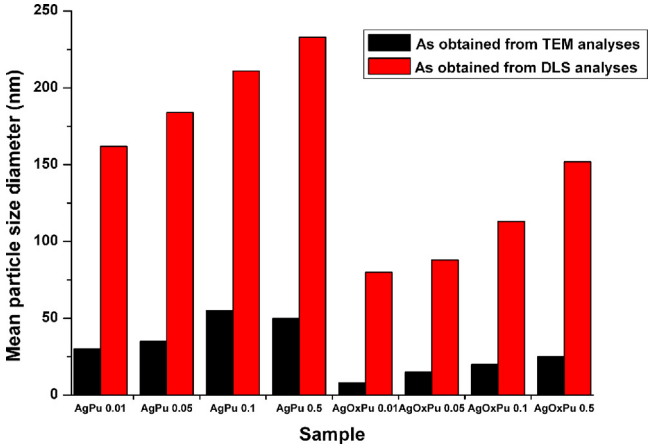

Fig. 6. Mean particle size diameter (nm) as obtained by TEM and DLS measurements for the pullulan and oxidized pullulan mediated silver nanoparticles.

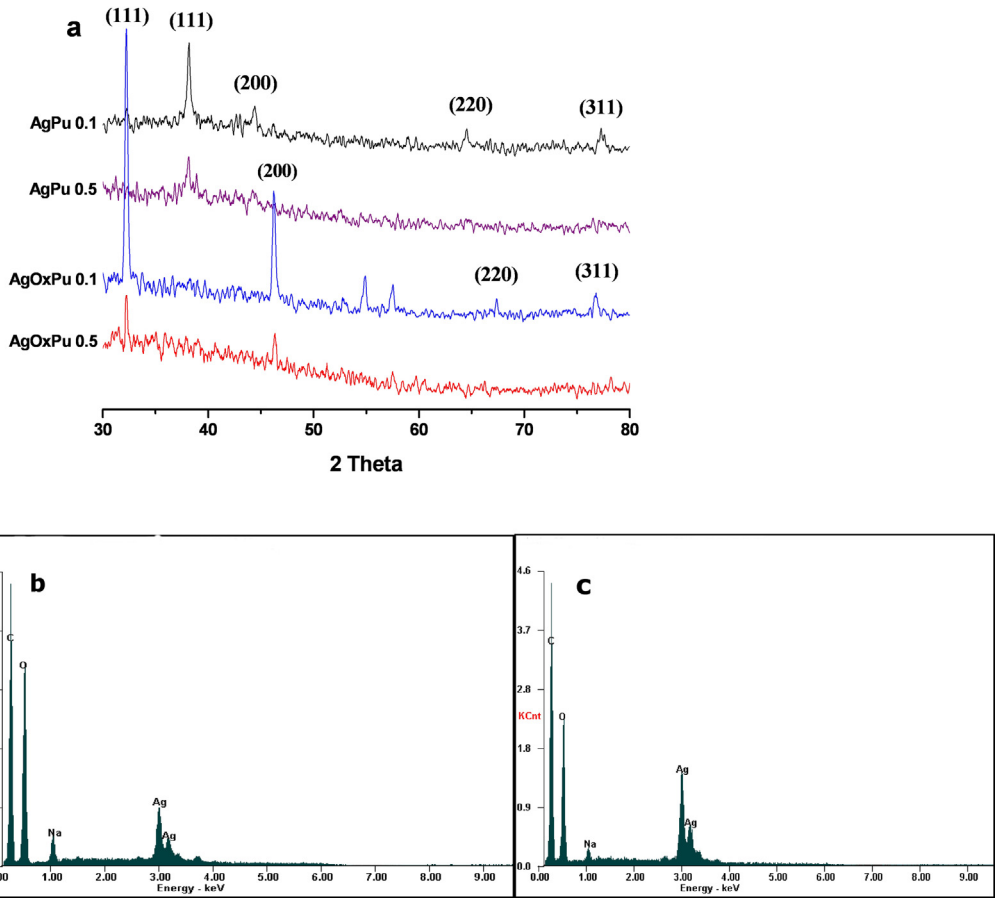

Fig. 7. X-ray diffraction pattern of pullulan/oxidized pullulan mediated silver nanoparticles (a) and EDX spectra of AgPu 0.5 sample (b) and AgOxPu 0.5 sample (c).

The pullulan and oxidized pullulan mediated silver nanoparticles were further analyzed by means of X-ray diffraction (XRD), in order to reveal the crystalline nature of those, Fig. 7. It can be seen, that the crystalline structure of silver nanoparticles is confirmed, since the typical XRD pattern of the AgNPs with four distinctive diffraction peaks in the 2 theta region are present: (1 1 1), (2 0 0), (2 2 0), and (3 1 1). These peaks are consistent with a face centered cubic (fcc) phase of Ag^0 standard (JCPDS Card no. 04-0783). The plane (1 1 1) presents the highest intensity as compared with the other planes, and the most interesting feature showed in Fig. 7a, is the difference occurred in the XRD patterns between the pullulan and 6-carboxypullulan used as mediators for the AgNPs, which suggest also differences on the silver capping by these two mediators (i.e. via hydroxyl groups in the case of pullulan and via both hydroxyl and carboxyl groups in the case of oxidized pullulan). Nevertheless, the entire XRD patterns are characteristic for the AgNPs and are in concordance with the previous published results in this field (Kanmani & Taik Lim, 2013; Bankura et al., 2012). However, in the sample AgOxPu 0.1, two additional peaks were observed with the Bragg peaks representative of fcc silver nanocrystals. These sharp peaks, at 2-theta values at ca. 55 and 58 could have resulted from crystallization of the reducing and stabilizing agent in the AgNPs, as have previously been observed by Bankura et al. (2012) and Roopan et al. (2013) in the case of using dextran and *Cocos nucifera* coir waste extract for preparation of AgNPs.

The analysis of the energy dispersive X-ray (XRD) spectroscopy can offer valuable information regarding the quantitative and qualitative presence of the elemental silver involved in the synthesis of the nanoparticles. Fig. 7b and c pointed out the presence of elemental silver in XRD spectra of AgPu 0.5 and AgOxPu 0.5 samples, confirmed by the strong peak at ~3 keV. Bankura et al. (2012) have also reported the presence of ~3 keV peak signal in the silver region for the dextran-stabilized silver nanoparticles. This is a clear indication of the silver nanoparticles formation in the reaction medium. Moreover, the presence of C, and O elements also proves that the nanocomposite consist on polysaccharide (pullulan or oxidized pullulan) and silver nanoparticles.

The FTIR spectra of pullulan, oxidized pullulan and pullulan/oxidized pullulan nanoparticles are presented in Fig. 8 and also in the Supplementary data associated with this paper.

Unoxidized pullulan shows typical FTIR spectrum for this kind of polysaccharide: a broad adsorption between 3000 and 3600 cm^{-1} region due to OH stretching vibration, centered around 3423 cm^{-1}, a band at 2926 cm^{-1} corresponding to the C—H stretching vibration, adsorption bands at 1458 cm^{-1} assigned to symmetric CH_2 bending vibration and 930 cm^{-1} assigned to C—O—C stretching at α-(1 → 4)-glycosidic linkages, a marker sign of "amorphous" region (Ciolacu, Ciolacu, & Popa, 2011). Moreover, the absorption peak at 1653 cm^{-1} indicated the presence of the carbonyl (C=O) stretching frequency (Kanmani & Taik Lim, 2013). After oxidation, some changes in the FTIR spectra appears, the most notable being the presence of one sharp and intense band at 1608 cm^{-1}, assigned to the C=O asymmetrical stretching of the free carboxylate groups introduced into the pullulan structure, whereas the adsorption band at 1418 cm^{-1} represents the C—O symmetric stretching of dissociated carboxyl groups (Saito et al., 2009).

After incorporating the silver nanoparticles into the pullulan, the FTIR spectrum of resulted product, differ on that of native pullulan; the OH stretching vibration band (centered at 3423 cm^{-1} in pullulan) shifted to 3438 cm^{-1} in the case of pullulan nanoparticles, Fig. 8, as well as the band from 1653 cm^{-1} was shifted to lower wave numbers. The strong interaction between pullulan

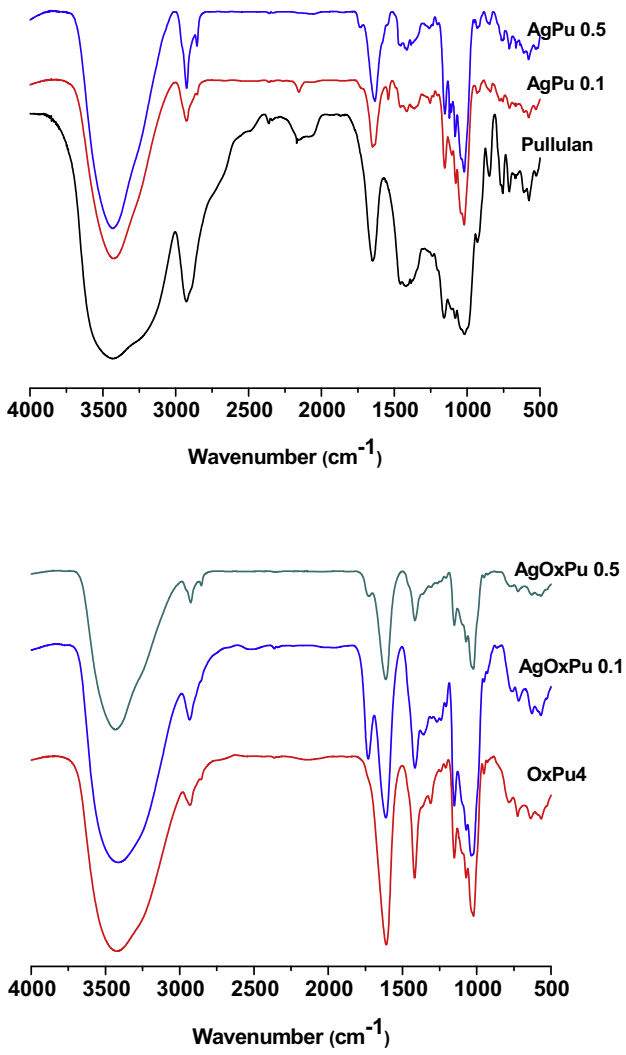

Fig. 8. FTIR spectra of pullulan, oxidized pullulan, and their silver nanoparticles.

and silver nanoparticles could be better evidenced by calculating the FT-IR peak area ratio (ν 3423/ν 1653 cm^{-1}) for pullulan and FT-IR peak area ratios (ν 3438/ν 1636 (1639) cm^{-1}) for the AgPu samples. This ratio increases from 2.24 in native pullulan, to 3.11 in AgPu 0.01 sample, 3.23 in AgPu 0.05 sample, 3.27 in AgPu 0.1 sample, and 3.33 in AgPu 0.5 sample, respectively. The IR absorption for ν_s C=O (1418 cm^{-1}) and ν_{as} C=O (1608 cm^{-1}) of deprotonated carboxylic acid group are observed in the spectra of oxidized pullulan-mediated silver nanoparticles, but their intensities are visibly decreased. These findings are supporting the binding of carboxylic groups with Ag nanoparticles through free carboxylate group (Shankar, Ahmad, & Sastry, 2003). Similarly, the FT-IR peak area ratio (ν 3420/ν 1608 cm^{-1}) for oxidized pullulan and FT-IR peak area ratios (νOH/ν_{as}C=O) for the AgOxPu samples were calculated. Again, the ratio increases from 1.08 in oxidized pullulan, to 1.10 in AgOxPu 0.01 sample, 1.22 in AgOxPu 0.05 sample, and 1.77 for both AgOxPu 0.1 and AgOxPu 0.5 samples. These results strongly suggest that the ν_{as}C=O peak intensities decreases due to their interaction with silver. Interestingly, in the spectra of oxidized pullulan nanoparticles a new adsorption band as a shoulder, around 1736 cm^{-1}, appears due to carboxylate groups which are involved in the attachment of silver atoms. Also the specific absorption peak at 1384 cm^{-1} of silver nanoparticles can be seen on the FTIR spectra.

Table 2
Mean ZOI values against *S. aureus* and *E. coli* (mm).

Sample code	*S. aureus* (mm)	*E. coli* (mm)
AgPu 0.1	8.6	9.4
AgPu 0.5	9.7	10.8
AgOxPu 0.1	12.3	9.8
AgOxPu 0.5	14.8	11.4

3.3. Antimicrobial activity against microorganism

Freshly prepared silver nanoparticles were further employed to test their antimicrobial activity against Gram-positive *S. aureus* ATCC 29213 and Gram-negative *E. coli* ATCC 25922. Both test organisms have multiresistant strains (MRSA, VREC), which often cause problems in the course of medical interventions. Although those multiresistant pathogens are not more virulent than their "common" congeners, a treatment using broadband antibiotics often fails which can lead to amputation of limbs and in severe cases even to death. In contrast, there are hardly any strains known that develop resistances towards silver based products due to different modes of action of silver against these pathogens.

In this paper, we use commonly employed ZOI tests in order to elucidate the antimicrobial activity of the silver nanoparticles. After 24 h of incubation at 37 °C, growth suppression was observed in plates loaded with 5 μg of silver nanoparticles. The diameter of the zone of inhibition (ZOI) in millimeters was measured. The mean ZOI of the triplicates of diameter are tabulated in Table 2.

The ZOI of around 15 mm and 10 mm, respectively, was observed for the Gram-positive bacterial strain *S. aureus* ATCC 29213 for AgOxPu 0.5 and AgPu 0.5. In the case of Gram-negative bacterial strains *E. coli* ATCC 25922 the detected ZOI were quite similar for the samples studied, with a maximum value of 11.4 for the AgOxPu 0.5. Based on these results, it can be concluded that both pullulan and oxidized pullulan nanoparticles had significant antibacterial action on a large variety of bacteria ranged from Gram-positive to Gram-negative ones. Similar results were found by Priyadharshini, Gopinath, Meera Priyadharsshini, MubarakAli, and Velusamy (2013) against Gram positive bacteria *B. cerus* and *Streptococcus pyogenes* and Gram negative bacterium *E. coli*, this behavior being linked with the tick cell wall of bacteria. Gram positive bacterial strains posses a three-dimensional thick layer of ~20–80 nm composed on linear polysaccharide chains cross linked by more short peptides (peptidoglycan layer) which is arduous to be penetrate by AgNPs. In the case of Gram negative bacteria, the peptidoglycan layer is only ~7–8 nm thick, being much more accessible for AgNPs (Priyadharshini et al., 2013). This explanation is in accordance with our results for the uncharged pullulan based nanoparticles, Table 2. However, highly negative charged oxidized pullulan based nanoparticles, exhibit a stronger affinity toward Gram positive bacteria, due to their attachment on the positive surface of bacteria, which induces changes on the morphology of the bacteria membrane, by affecting respiration processes and cell division, leading eventually to the perish of the cell, (Gonzáles-Campos et al., 2013). It is important to point out the exceptional activity of the oxidized pullulan nanoparticles against Gram-positive bacterial strains compared with other Gram-negative strains in this antibacterial susceptibility assay, which can be explained by the highly negative zeta potential value of the mentioned silver nanoparticles. Negatively charged OxPu nanoparticles can attach to the positively charged bacterial cell surface and interrupt the membrane's functionality according with the two mechanisms: (i) by causing an effusion of the intracellular components, or (ii) by inhibiting the transport of nutrients into cells. (Helander, Nurmiaho-Lassila, Ahvenainen, Rhoades, & Roller, 2001). Conversely, positive charged chitosan silver nanocomposites were found to be more effective

toward Gram negative bacteria strains, due to their positive charge conferred by chitosan, which enhances the binding ability to negative charges on the cell surface (Gonzáles-Campos et al., 2013).

4. Conclusions

A simple, safe, one-step, *environment-friendly* method for the preparation of silver nanoparticles in aqueous solutions of pullulan or oxidized pullulan at room temperature is reported. Both used polysaccharides act as a reducing and stabilizing agent for the synthesis of silver nanoparticles. The stability of the prepared nanoparticles depends on the biopolymers structure used for capping silver atoms, and range from three months (for the pullulan nanoparticles) to more than six months for the oxidized pullulan nanoparticles. All the freshly prepared nanoparticles showed excellent antibacterial activity against different types of bacteria, activity which can be correlated with the zeta potential value of the samples. The oxidized pullulan mediated silver nanoparticles, due to their higher negative values of the zeta potential, acquire an increased stability due to repulsion among the particles, as well as exhibit a strong antibacterial activity against Gram positive bacteria strains.

Acknowledgment

The authors gratefully acknowledge to the Acad. Professor Bogdan C. Simionescu for providing the all laboratory facilities and fruitful discussions.

Appendix A. Supplementary data

Supplementary data associated with this article can be found, in the online version, at http://dx.doi.org/10.1016/j.carbpol.2014.06.008.

References

Alayoglu, S., Nilekar, A. U., Mavrikakis, M., & Eichhorn, B. (2008). Ru@Pt core–shell nanocatalysts for enhanced preferential oxidation of CO in hydrogen. *Nature Material*, *7*, 333–338.

Aslan, K., Lakowicz, J. R., & Geddes, C. D. (2005). Plasmon light scattering in biology and medicine: New sensing approaches, visions and perspectives. *Current Opinions in Chemical Biology: Analytical Techniques*, *9*, 538–544.

Bankura, K. P., Maity, D., Mollick, M. M. R., Mondal, D., Bhowmick, B., Bain, M. K., et al. (2012). Synthesis, characterization and antimicrobial activity of dextran stabilized silver nanoparticles in aqueous medium. *Carbohydrate Polymers*, *89*, 1159–1165.

Breitwieser, D., Moghaddam, M. M., Spirk, S., Baghbanzadeh, M., Pivec, T., Fasl, H., et al. (2013). In situ preparation of silver nanocomposites on cellulosic fibers-microwave vs. conventional heating. *Carbohydrate Polymers*, *94*, 677–686.

Ciolacu, D., Ciolacu, F., & Popa, V. I. (2011). Amorphous cellulose—Structure and characterization. *Cellulose Chemistry and Technology*, *45*, 13–21.

Gao, F. P., Zhang, H. Z., Liu, L. R., Wang, Y. S., Jiang, Q., Yang, X. D., et al. (2008). Preparation and physicochemical characterization of self-assembled nanoparticles of deoxycholic acid modified-carboxymethylcurdlan conjugates. *Carbohydrate Polymers*, *71*, 606–613.

Garciá-Barrasa, J., López-de-Luzuriaga, J. M., & Monge, M. (2011). Silver nanoparticles: Synthesis through chemical methods in solution and biomedical applications. *Central European Journal of Chemistry*, *9*, 7–19.

Giorgetti, E., Giusti, A., Laza, S. C., Marsili, P., & Giammanco, F. (2007). Production of colloidal gold nanoparticles by picosecond laser ablation in liquids. *Physica Status Solidi A*, *204*, 1693–1698.

Goia, D. V. (2004). Preparation and formation mechanisms of uniform metallic particles in homogeneous solutions. *Journal of Material Chemistry*, *14*, 451–458.

Gonzáles-Campos, J. B., Mota-Morales, J. D., Kumar, S., Zárate-Triviño, D., Hernández-Iturriaga, M., Prokhorov, Y., et al. (2013). New insights into the bactericidal activity of chitosan–Ag bionanocomposite: The role of the electrical conductivity. *Colloids and Surfaces B: Biointerfaces*, *111*, 741–746.

Helander, I. M., Nurmiaho-Lassila, E. L., Ahvenainen, R., Rhoades, J., & Roller, S. (2001). Chitosan disrupts the barrier properties of the outer membrane of Gram-negative bacteria. *International Journal of Food Microbiology*, *71*, 235–244.

Huang, H., & Yang, X. (2004). Synthesis of polysaccharide-stabilized gold and silver nanoparticles: A green method. *Carbohydrate Research*, *339*, 2627–2631.

Ifuku, S., Tsuji, M., Morimoto, M., Saimoto, H., & Yano, H. (2009). Synthesis of silver nanoparticles templated by TEMPO-mediated oxidized bacterial cellulose nanofibers. *Biomacromolecules*, *10*, 2714–2717.

Kanmani, P., & Lim, S. T. (2013). Synthesis and characterization of pullulan-mediated silver nanoparticles and its antimicrobial activities. *Carbohydrate Polymers*, *97*, 421–428.

Kaya, A., Du, X., Liu, Z., Lu, J. W., Morris, J. R., Glasser, W. G., et al. (2008). Surface plasmon resonance studies of pullulan and pullulan cinnamate adsorption onto cellulose. *Biomacromolecules*, *10*, 2451–2459.

Khan, Z., Al-Thabaiti, S. A., Obaid, A. Y., & Al-Youbi, A. O. (2011). Preparation and characterization of silver nanoparticles by chemical reduction method. *Colloids and Surface B: Biointerfaces*, *82*, 513–517.

Khorsand Zak, A., Razali, R., Abd Majid, W. H., & Darroudi, M. (2011). Synthesis and characterization of a narrow size distribution of zinc oxide nanoparticles. *International Journal of Nanomedicine*, *6*, 1399–1403.

Ko, T. S., Yang, S., Hsu, H. C., Chu, C. P., Lin, H. F., Liao, S. C., et al. (2006). ZnO nanopowders fabricated by dc thermal plasma synthesis. *Materials Science and Engineering B*, *134*, 54–58.

Kowlgi, K., Lafont, U., Rappolt, M., & Koper, G. (2012). Uniform metal nanoparticles produced at high yield in dense microemulsions. *Journal of Colloid and Interface Science*, *372*, 16–23.

Pandey, S., Goswami, G. K., & Nanda, K. K. (2012). Green synthesis of biopolymer–silver nanoparticle nanocomposite: An optical sensor for ammonia detection. *International Journal of Biological Macromolecules*, *51*, 583–589.

Paris, E., & Stuart, M. A. C. (1999). Adsorption of hydrophobically modified 6-carboxypullulan on a hydrophobic surface. *Macromolecules*, *32*, 462–470.

Pereira, J. M., Mahoney, M., & Edgar, K. J. (2014). Synthesis of amphiphilic 6-carboxypullulan ethers. *Carbohydrate Polymers*, *100*, 65–73.

Pimpang, P., Sutham, W., Mangkorntong, N., Mangkorntong, P., & Choopun, S. (2008). Effect of stabilizer on preparation of silver and gold nanoparticle using grinding method. *Chiang Mai Journal of Science*, *35*, 250–257.

Priyadharshini, S., Gopinath, V., Meera Priyadharsshini, N., Mubarak Ali, D., & Velusamy, P. (2013). Synthesis of anisotropic silver nanoparticles using novel strain, Bacillusflexus and its biomedical application. *Colloids and Surfaces B: Biointerfaces*, *102*, 232–237.

Raveendran, P., Fu, J., & Wallen, S. L. (2003). Completely green synthesis and stabilization of metal nanoparticles. *Journal of the American Chemical Society*, *125*, 13940–13941.

Roopan, S. M., Rohit Madhumitha, G., Abdul Rahumanb, A., Kmaraj, C., Bharathi, A., & Surendra, T. V. (2013). Low-cost and eco-friendly phyto-synthesis of silver nanoparticles using *Cocos nucifera* coir extract and its larvicidal activity. *Industrial Crops and Products*, *43*, 631–635.

Saito, T., Hirota, M., Tamura, N., Fukuzumi, H., Kimura, S., Heux, L., et al. (2009). Individualization of nano-sized plant cellulose fibrils by direct surface carboxylation using TEMPO catalyst under neutral conditions. *Biomacromolecules*, *10*, 1992–1996.

Salah, N., Habib, S. S., Khan, Z. H., Memic, A., Azam, A., Alarfaj, E., et al. (2011). High-energy ball milling technique for ZnO nanoparticles as antibacterial material. *International Journal of Nanomedicine*, *6*, 863–869.

Sapsford, K. E., Pons, T., Medintz, I. L., & Mattoussi, H. (2006). Biosensing with luminescent semiconductor quantum dots. *Sensors*, *6*, 925–953.

Shankar, S. S., Ahmad, A., & Sastry, M. (2003). Geranium leaf assisted biosynthesis of silver nanoparticles. *Biotechnology Progress*, *19*, 1627–1631.

Sharmaa, D., Sharmab, S., Kaitha, B. S., Rajputa, J., & Kaurb, M. (2011). Synthesis of ZnO nanoparticles using surfactant free in-air and microwave method. *Applied Surface Science*, *257*, 9661–9672.

Song, K. C., Lee, S. M., Park, T. S., & Lee, B. S. (2009). Preparation of colloidal silver nanoparticles by chemical reduction method. *Korean Journal of Chemical Engineering*, *26*, 153–155.

Spatareanu, A., Bercea, M., Budtova, T., Harabagiu, V., Sacarescu, L., & Coseri, S. (2014). Synthesis, characterization and solution behaviour of oxidized pullulan. *Carbohydrate Polymers*, *111*, 63–71.

Tran, H. V., Tran, L. D., Ba, C. T., Vu, H. D., Nguyen, T. N., Pham, D. G., & Nguyen, P. X. (2010). Synthesis, characterization, antibacterial and antiproliferative activities of monodisperse chitosan-based silver nanoparticles. *Colloids and Surfaces A: Physicochemical and Engineering Aspects*, *360*, 32–40.

Turner, S., Tavernier, S. M. F., Huyberechts, G., Biermans, E., Bals, S., Batenburg, K. J., & Tendeloo, G. (2010). Assisted spray pyrolysis production and characterization of ZnO nanoparticles with narrow size distribution. *Journal of Nanoparticle Research*, *12*, 615–622.

Twu, Y. K., Chen, Y. W., & Shih, C. M. (2008). Preparation of silver nanoparticles using chitosan suspensions. *Powder Technology*, *185*, 251–257.

Wu, S., Sun, A., Zhai, F., Wang, J., Xu, W., Zhang, Q., & Volinsky, A. A. (2011). Fe_3O_4 magnetic nanoparticles synthesis from tailings by ultrasonic chemical co-precipitation. *Materials Letters*, *65*, 1882–1884.

Xu, J., Yang, H., Fu, W., Du, K., Sui, Y., Chen, J., et al. (2007). Preparation and magnetic properties of magnetite nanoparticles by sol–gel method. *Journal of Magnetism and Magnetic Materials*, *309*, 307–311.

Zschech, D., Ha Kim, D., Alexey, P., Hopfe, S., Scholz, R., Goring, P., et al. (2006). High-temperature resistant, ordered gold nanoparticle arrays. *Nanotechnology*, *17*, 2122–2126.